J. Biochem. 2011;150(4):461–471 doi:10.1093/jb/mvr081

JB THE JOURNAL OF BIOCHEMISTRY

Cellular responses induced by cerium oxide nanoparticles: induction of intracellular calcium level and oxidative stress on culture cells

Received April 4, 2011; accepted June 5, 2011; published online June 21, 2011

Masanori Horie[1,*,†], Keiko Nishio[1], Haruhisa Kato[2], Katsuhide Fujita[3], Shigehisa Endoh[4], Ayako Nakamura[2], Arisa Miyauchi[4], Shinichi Kinugasa[2], Kazuhiro Yamamoto[5], Etsuo Niki[1], Yasukazu Yoshida[1], Yoshihisa Hagihara[1] and Hitoshi Iwahashi[1]

[1]Health Research Institute, National Institute of Advanced Industrial Science and Technology (AIST), 1-8-31, Midorigaoka, Ikeda, Osaka 563-8577; [2]National Metrology Institute of Japan (NMIJ), AIST, 1-1-1 Higashi, Tsukuba, Ibaraki 305-8565; [3]Research Institute of Science for Safety and Sustainability (RISS), AIST, 16-1 Onogawa, Tsukuba, Ibaraki 3058569; [4]Research Institute for Environmental Management Technology (EM-TECH), AIST, Particle Measurement Group, 16-1 Onogawa; and [5]Research Institute of Instrumentation Frontier (RIIF), AIST, 1-1-1 Umezono, Tsukuba, Ibaraki, 305-8565, Japan

*Present address: Masanori Horie, Institute of Industrial Ecological Sciences, University of Occupational and Environmental Health, Kitakyushu, Fukuoka 807-8555, Japan.

†Masanori Horie, Institute of Industrial Ecological Sciences, University of Occupational and Environmental Health, Kitakyushu, Fukuoka 807-8555, Japan. Tel: +81 (0)93 691 4284, Fax: +81 (0)93 691 7466, email: masa-horie@med.uoeh-u.ac.jp

Cerium oxide (CeO_2) is an important metal oxide used for industrial products. Many investigations about the cellular influence of CeO_2 nanoparticles have been done, but results are contradictory. It has been reported that CeO_2 nanoparticles have an anti-oxidative effect in cells, but it has also been reported that CeO_2 nanoparticles induce oxidative stress. We investigated the potential influence on cells and the mechanisms induced by CeO_2 nanoparticles *in vitro*. We prepared a stable CeO_2 culture medium dispersion. Cellular responses in CeO_2 medium-exposed cells were examined. Cellular uptake of CeO_2 nanoparticles was observed. After 24-h exposure, a high concentration of CeO_2 nanoparticles (~200 mg/ml) induced an increase in the intracellular level of reactive oxygen species (ROS); a low concentration of CeO_2 nanoparticles induced a decrease in the intracellular ROS level. On the other hand, exposure of CeO_2 nanoparticle for 24 h had little influence on the cell viability. Exposure of CeO_2 nanoparticles increased the intracellular Ca^{2+} concentration and also Calpain was activated. These results suggest that CeO_2 nanoparticles have a potential to induce intracellular oxidative stress and increase the intracellular Ca^{2+} level, but these influences are small.

Keywords: Oxidative stress/Endocytosis/New Effects of Biomaterials/Radicals/Toxicity.

Abbreviations: DCFH-DA, 2′,7′-dichlorofluorescin diacetate; DLS, dynamic light scattering; DMEM, Dulbecco's modified Eagle medium; FBS, foetal bovine serum; ROS, reactive oxygen species.

Cerium oxide (ceria; cerium dioxide; CeO_2) has been widely used for various industrial materials (polishing agents and fuel additives) as well as for catalysis in industrial reactions. Recently, the production of nanoparticles (defined as particles in which at least one dimension is $\leq$100 nm) has been increasing.

Nanoparticles have superior physical and chemical properties for industrial use than fine-scale particles because of the increase in surface area per weight. These properties may be beneficial in industry, but they also may affect animals, humans and the environment. Some metal oxide nanoparticles such as CuO, NiO and ZnO are strongly cytotoxic (*1–4*).

There are investigations on focus of the influence of CeO_2 nanoparticles on living cells, but results from different studies contradicted each other. A study of an energy-efficient diesel fuel additive that included CeO_2 nanoparticles showed that it did not influence biological responses such as induction of oxidative stress and inflammation (*5*, *6*). CeO_2 nanoparticles were not mutagenic to bacteria (*6*) and CeO_2 nanoparticles did not injure DNA and chromatin in human cells (*7*). Some investigations indicated that CeO_2 nanoparticles had anti-oxidative activity and protected rodent nerve cells and human bronchial cells from oxidative stress (*8*, *9*). CeO_2 nanoparticles showed superoxide dismutase (SOD)-like activity and protected cells from oxidative stress (*10*). CeO_2 nanoparticles have a potential to reduce the production of reactive oxygen species (ROS) in macrophages (*11*). Exposure of CeO_2 nanoparticles to epithelial cells induced induction of the anti-oxidant enzyme HO-1 via the Nrf-2 pathway (*12*). In these investigations, CeO_2 nanoparticles were not toxic. The results suggested that CeO_2 nanoparticles are beneficial for human health due to their anti-oxidative activity. In contrast, it has also been reported that CeO_2 nanoparticles induce oxidative stress and subsequent cytotoxicity in cells (*13*, *14*). Moreover, CeO_2 nanoparticles attacked the outer membrane of *Escherichia coli* cells and showed a lethal effect (*15*). These conflicting results may limit the use of CeO_2 nanoparticles. Understanding the true

biological influence of CeO_2 nanoparticles is therefore important.

In all of above results, oxidative stress was an important factor. In fact, oxidative stress is also an important factor for human health. Strong and sustained oxidative stress leads to increase in the risk of cancer, cardiovascular disease or neurological disease. Conversely, mild oxidative stress can induce beneficial effects such as activation of defense systems as 'eustress' (*16*). Hence, understanding the association between oxidative stress and cellular responses is important for risk assessment.

As described previously, some metal oxide nanoparticles such as CuO and ZnO induce strong oxidative stress in cells (*4*, *9*). In many cases, metal oxide nanoparticles that show oxidative stress-related cytotoxicity are soluble in the culture medium and the cytotoxicity is caused by the release of metal ions. In general, CeO_2 particles are insoluble in water. CeO_2 nanoparticles show strong adsorption of protein and calcium ions (Ca^{2+}) (*17*). We reported that the adsorption of components of the culture medium to CeO_2 nanoparticles induce artificial cytotoxicity *in vitro* due to medium depletion. However, the influence of adsorbed materials on the surface of CeO_2 nanoparticle on cells is unclear.

In the present study, cellular responses induced by CeO_2 nanoparticles were examined. We particularly focused on oxidative stress and also examined the influence of adsorbed Ca^{2+} on CeO_2 nanoparticles and the possible mechanisms underlying this process.

Materials and Methods

Cell culture

Human keratinocyte HaCaT cells were purchased from the German Cancer Research Center (DKFZ, Heidelberg, Germany). Human lung carcinoma A549 cells were purchased from the RIKEN BioResource Center (Tsukuba, Ibaraki, Japan).

Cells were cultured in Dulbecco's modified Eagle's medium (DMEM) (Gibco, Invitrogen Corporation, Grand Island, NY, USA) supplemented with 10% heat-inactivated foetal bovine serum (FBS) (CELLect GOLD; MP Biomedicals Incorporated, Solon, OH, USA), 100 U/ml penicillin, 100 µg/ml streptomycin and 250 ng/ml amphotericin B (Nacalai Tesque Incorporated, Kyoto, Japan). In the present study, this DMEM preparation is referred to as 'DMEM–FBS'. Cells in DMEM–FBS were placed in 75-cm^2 flasks (Corning Incorporated, Corning, NY, USA) and cultured at 37°C in an atmosphere of 5% CO_2. For examinations, cells were seeded in 96-well plates (for cell viability assays) or 6-well plates (for other assays) at 2×10^5 cells/ml and incubated for 24 h. For confocal laser microscope observation, cells were seeded in glass bottom dishes (Matsunami Glass Ind. Ltd., Kishiwada, Japan). Subsequently, the culture medium was exchanged for CeO_2–DMEM–FBS dispersion medium and cells cultured for another 2, 6, 12 or 24 h.

Preparation of CeO_2-medium dispersions

CeO_2 nanoparticles were purchased from C. I. Kasei Company, Limited (Tokyo, Japan). Particles were produced by physical vapour synthesis (PVS). Fine CeO_2 particles were purchased from Junsei Chemical Company, Limited (Tokyo, Japan). Properties of primary particles are shown in Table I. Their specific surface areas were measured by the Brunauer–Emmett–Teller (BET) method. A stable and uniform dispersion was prepared by pre-adsorption and centrifugation.

A CeO_2 nanoparticle induces medium depletion due to its adsorption ability (*17*). To prevent cell starvation because of adsorption of medium components onto the surface of CeO_2 particles, the protein adsorption ability of CeO_2 nanoparticles was saturated by pre-treatment with FBS. CeO_2 particles were dispersed in 80 mg/ml FBS. The dispersion was subsequently centrifuged at 16,000*g* for 20 min. Precipitated CeO_2 particles were washed with FBS-free DMEM and redispersed in an equivalent volume of fresh DMEM–FBS. The secondary particle size in the dispersion was made uniform by step-wise centrifugation. The dispersion of nanoparticles in DMEM–FBS was centrifuged at 8,000*g* for 20 min. After discarding the supernatant, the precipitate was resuspended in an equal volume of fresh DMEM–FBS. The resulting CeO_2 dispersion was centrifuged at 4,000*g* for 20 min. The process described above was repeated until the supernatant collected became a uniform and stable CeO_2 dispersion. Centrifugal force was gradually reduced from 2,000*g* to 1,000*g*. The dispersion of fine particles was prepared following the same procedure described above, but with centrifugation carried out at 500*g*. Fractions of CeO_2 nanoparticles centrifuged at 4000*g* and 1000*g* were used for evaluation of cellular responses.

Table I. Properties of CeO_2 primary particles.

	Primary particle size[a] (nm)	Purity[a] (%)	Specific surface area (m^2/g) Manufacturer's data[a]	BET multi points	BET single point
Nano-CeO_2	14	>99.8	61.0	55.9	55.6
Fine-CeO_2	400	99.9	69.2	153.6	150.3

[a]According to manufacturer's data sheets. Other data were measured in this study.

Characterization of CeO_2-medium dispersions

In the present study, a 'secondary particle' was defined as a complex aggregate of primary particles, proteins from FBS and other medium components. 'Average particle size' was defined as the size of secondary particles as estimated from light-intensity measurements assuming that the aggregate was globular. The CeO_2–DMEM–FBS dispersion prepared via the aforementioned method was divided into three parts. These parts were used to carry out simultaneous biological examinations and to take measurements of the concentration and particle size of CeO_2.

The secondary particle size in the CeO_2–DMEM–FBS dispersion was measured by dynamic light scattering (DLS). Details of this experiment are described elsewhere (*18*, *19*). The estimated diameter of a secondary particle was the mean of three measurements using: a homodyne DLS particle analyser (DLS7000, Otsuka Electronics Company, Limited, Hirakata, Japan) with a goniometre system and a 35-mW He–Ne laser at a wavelength of 632.8 nm; a fiberoptic particle analyser (FPAR1000, Otsuka Electronics Company, Limited) with a 5-mW semiconductor laser at a wavelength of 658 nm and a heterodyne DLS particle analyser (Nanotrac UPA 151, Microtrac Incorporated, Montgomeryville, PA, USA) with a 3-mW semiconductor laser at a wavelength of 780 nm. Samples for measurement of particle size and cytotoxicity assay were obtained at 1 cm from the surface of the solutions in a static 15-ml tube. CeO_2 concentration was measured by X-ray fluorescence (XRF) analyses. Briefly, 13 ml of metal oxide–DMEM–FBS dispersion was added to 13 ml of a standard solution (including 0.1 mg/ml of Fe as an internal standard element) and mixed well. Then, 5 ml of the mixture was dried in an oven at 200°C for 24 h. A dried sample was ground in an agate mortar. XRF was done using a dispersive X-ray fluorescence spectrometer JSX-3201 (Jeol Limited, Tokyo, Japan). The amount of cerium was estimated from the molar ratio of cerium and the internal standard. The specific surface areas were measured by the BET method.

Determination of the viability and proliferation of cells

Two assays were conducted for cytotoxicity determination: 3-(4,5-dimethyl-2-thiazolyl)-2,5-diphenyltetrazolium bromide (MTT) assay and lactate dehydrogenase (LDH) assay.

In MTT assays, cells were incubated with 0.5 mg/ml MTT (Nacalai Tesque Incorporated) at 37°C for 2 h. Next, isopropyl alcohol containing 40 mM HCl was added to the culture medium

(3:2 v/v) and mixed with a pipette until the formazan had completely dissolved. The optical density of the formazan was measured at 570 nm using a Multiskan Ascent plate reader (Thermo Labsystems, Helsinki, Finland).

In LDH assays, LDH release was measured with tetrazolium salt using a cytotoxicity detection kit^{PLUS} (LDH) (Roche Diagnostics GmbH, Mannheim, Germany) according to the manufacturer's protocol. Cytotoxicity was calculated as follows:

$$\text{Cytotoxicity}\,(\%) = (\text{experimental value} - \text{low control})/(\text{high control} - \text{low control}) \times 100. \quad (1)$$

The low control (refers to the spontaneous release of LDH) was determined as the LDH released from untreated normal cells. The high control (refers to the maximum release of LDH) was determined as the LDH released from cells lysed by a solution provided in the kit.

Colony-forming ability (i.e. cell proliferation) was detected by a clonogenic assay based on the methods of Herzog *et al.* (*20*) and Franken *et al.* (*21*). Briefly, cells were seeded in six-well microplates (Corning Incorporated) at 300 cells per well. Cells were allowed to attach for ~14 h and treated with 2 ml of CeO_2–DMEM–FBS dispersions from the dispersions. Cells were then cultured for the time period required for control cells to form colonies (one colony was defined as ≤50 cells), i.e. 7 days. After completion of the culture procedure, the dispersions were removed and cells washed with 2 ml phosphate-buffered saline (PBS). After fixation with 100% methanol for 15 min, cells were stained with Giemsa solution (Nacalai Tesque Incorporated) diluted 1:50 in water for 15 min and rinsed with distilled water. The number of colonies was counted.

Assay for caspase-3 activity

To obtain total cell extracts, CeO_2-treated cells were first collected by 0.25% trypsinization. They were then washed with cold PBS and resuspended on ice for 10 min in lysis buffer (150 mM NaCl, 50 mM Tris–HCl, pH 7.4), 50 mM NaF, 5 mM ethylenediamine tetra-acetic acid (EDTA), 0.5% Triton X-100 and 1 mM Na_3VO_4, along with a protease inhibitor cocktail tablet (Roche Diagnostics). Nuclei and non-lysed cellular debris were removed by centrifugation at 10,000*g* for 1 min.

Protein concentration was determined by the bicinchoninic acid (BCA) method using BCA protein assay kit (Thermo Fisher Scientific Incorporated, Rockford, IL, USA) with bovine serum albumin as a standard. Caspase-3 activity was measured by cleavage of the Asp–Glu–Val–Asp (DEVD) peptide-conjugated 7-amino-4-trifluoromethyl coumarin (AFC), according to the protocol outlined by the manufacturer of the caspase-3 fluorometric protease assay kit (Medical and Biological Laboratories Company Limited, Nagoya, Japan). Substrate cleavage, which resulted in the release of AFC fluorescence (excitation, 400 nm; emission, 505 nm), was measured using a Fluoroskan Ascent CF plate reader (Thermo Labsystems).

Measurement of the level of intracellular ROS and hydroperoxide

Intracellular ROS were detected using dichlorofluorescin diacetate (DCFH-DA; Sigma–Aldrich, St Louis, MO, USA). DCFH-DA was dissolved in dimethyl sulfoxide (DMSO) at 5 mM as a stock solution and stored at −20°C. After incubation of cells with the CeO_2–DMEM–FBS dispersions, the dispersion was changed to serum-free DMEM containing 10 μM of DCFH-DA and incubated for 30 min at 37°C. Cells were then washed once with PBS, collected by 0.25% trypsinization, washed again with PBS and resuspended in 500 μl of PBS. Cell samples in PBS were excited with a 488-nm argon laser in the Cytomics FC500 flow cytometry system (Beckman Coulter Inc., Brea, CA, USA). The emission of 2′,7′-dichlorofluorescein (DCF) was recorded at 525 nm. Data were collected from at least 5,000 gated events.

Intracellular hydroperoxide was detected using diphenyl-1-pyrenylphosphine (DPPP; Dojindo Laboratories, Kumamoto, Japan) (*22*). DPPP was dissolved in DMSO at 5 mM as a stock solution and stored at −20°C. After incubation of cells for another 24 h with the CeO_2–DMEM–FBS dispersion, the medium was changed to serum-free DMEM containing 50 μM of DPPP and incubated for 30 min at 37°C. Cells were then washed with PBS, harvested by trypsinization, washed again with PBS and resuspended in 3 ml of PBS. Cell samples in PBS were excited with a 351-nm argon laser. The emission of DPPP oxide was measured at 380 nm using an RF-5300PC spectrofluorophotometer (Shimadzu Corporation, Kyoto, Japan). After measurement, cells were collected and measured for protein concentration. DPPP oxide fluorescence was normalized by cellular protein concentration.

Observation by transmission electron microscopy

CeO_2-exposed cell specimens were observed by transmission electron microscopy (TEM). TEM specimens were prepared as follows. Cells were fixed using 2.5% glutaraldehyde (TAAB Laboratories Equipment Ltd., Aldermaston, Berkshire, UK.) for 2 h at 4°C and 1% osmium tetroxide solution for 2 h at 4°C. They were then dehydrated in ethanol and embedded in epoxy resin. Ultra-thin sections were cut with a diamond knife with ultra-microtomy. TEM observations were achieved using an H-7000 transmission electron microscope (Hitachi, Tokyo, Japan). The acceleration voltage was 75 kV.

Determination of protein and Ca^{2+} concentration

CeO_2 particles were dispersed in DMEM–FBS at 1, 5, 10, 50 and 100 mg/ml and mixed well. Then particles were removed from the dispersion with centrifugation at 16000*g* for 20 min and the supernatant collected for the determination of the concentration of protein and Ca^{2+}.

The protein content of the culture medium was determined by the BCA method with bovine serum albumin as a standard. The Ca^{2+} content of the culture medium was determined by the *O*-cresolphthalein complexone (OCPC) colour development method using Wako calcium-C kit (Wako Pure Chemical Industries, Osaka, Japan). DMEM without serum and Ca^{2+} was used as a blank.

Measurement of the level of intracellular Ca^{2+}

Intracellular Ca^{2+} was detected using 1-[2-amino-5-(2,7-difluoro-6-hydroxy-3-oxo-9-xanthenyl)phenoxy]-2-(2-amino-5-methylphenoxy) ethane-N,N,N′,N′-tetraacetic acid, pentaacetoxymethyl ester (Fluo 4-AM; Dojindo Laboratories, Kumamoto, Japan).

Fluo 4-AM was dissolved in DMSO at 1 mg/ml as a stock solution and stored at −20°C. After incubation of cells with the CeO_2–DMEM–FBS dispersions, the dispersion was changed to Fluo 4-AM working solution [50 μl of Fluo 4-AM stock solution and 80 μl of 5% Pluronic F-127 (AnaSpec Incorporated, Fremont, CA, USA] in 10 ml of Hanks' buffered solution (Gibco) and incubated for 1 h at 37°C. Cells were then washed once with PBS, collected by 0.25% trypsinization, washed again with PBS and resuspended in 500 μl of PBS. Cell samples in PBS were excited with a 488-nm argon laser in a Cytomics FC500 flow cytometry system. The emission of Fluo 4 was recorded at 525 nm. Data were collected from at least 5,000 gated events.

For confocal laser microscope observation, after incubation of cells with the CeO_2–DMEM–FBS dispersions, the dispersion was changed to serum-free DMEM including 5 μg/ml of Fluo 4-AM and incubated for 1 h at 37°C. Cells were then washed once with PBS, DMEM–FBS was added and the fluorescence of Fluo-4 was observed by confocal laser microscope (Fluoview FV10i, Olympus Corporation, Tokyo, Japan). Observation was performed under excitation and emission wavelengths were 494 and 516 nm, respectively.

Assay for calpain activity

Calpain activity was measured using a calpain activity assay kit (Medical and Biological Laboratories Company Limited). Calpain activity was measured by cleavage of the calpain substrate Ac-LLY-conjugated AFC. After incubation of cells with the CeO_2–DMEM–FBS dispersions, cells were collected by 0.25% trypsinization. To obtain total cell extracts, CeO_2-treated cells pellet was then resuspended in 100 μl of extraction buffer (supplied by the manufacturer) and the cell suspension incubated on ice for 20 min. Non-lysed cellular debris were removed by centrifugation at 10,000*g* for 1 min. Protein concentration was determined using a BCA protein assay kit with bovine serum albumin as a standard. The cell lysate (including 100 μg of protein) was used for assay. The measurement of calpain activity was done according to the manufacturer's protocol.

Statistical analyses

Data are mean ± standard deviation from at least three separate experiments. Statistical analyses were done via an analysis of variance (ANOVA) using Dunnett's or Tukey tests for multiple comparisons. Calculation methods are described in each figure legend.

Results

Characterization of the CeO_2–DMEM–FBS dispersions

We prepared three types of CeO_2–DMEM–FBS dispersion. Each dispersion had a different size of primary or secondary particle. Details of the DLS measurement of CeO_2–DMEM–FBS dispersions are reported elsewhere (*19*).

Secondary particle sizes in CeO_2–DMEM–FBS dispersions were approximately 90–100 nm (4,000*g* preparation of nanoparticle dispersion), 130–150 nm (1000*g* preparation of nanoparticle dispersion) and 190 nm (500*g* preparation of fine-particle dispersion) as number-averaged particle size estimated from the light intensity of DLS. All of the dispersions were very stable for the experimental period employed. The light-scattering intensities of CeO_2 secondary nanoparticles did not change for at least 4 days. This observation indicated that there was no change in secondary particle size during the experimental period. Sedimentation of secondary particles was not observed. The concentration of CeO_2–DMEM–FBS dispersions therefore conformed to cell-exposure concentration. The specific surface areas of CeO_2 particles were also measured by the BET method (Table I). The specific surface area of CeO_2 nanoparticles measured in the present study was similar to the manufacturer's data. The specific surface area of CeO_2 fine particles was larger than the manufacturer's data. The specific surface area of fine-scale CeO_2 was larger than for nanoparticles. It can be supposed that the fine-scale CeO_2 particles used in the present study was porous. CeO_2 nanoparticles and CeO_2 fine particles did not dissolve in DMEM–FBS.

Influence of CeO_2 particles on cell viability

First, injury to the cell membrane due to exposure to CeO_2 was examined by the LDH assay (Fig. 1A). Cells exposed to nano-scale and fine CeO_2 particles did not show LDH leakage. Even if cells were exposed to intracellular oxidative-induced conditions (200 μg/ml of CeO_2 nanoparticles exposed for 24 h), LDH activity did not increase in the culture supernatant. The MTT assay was also carried out (Fig. 1B). Mitochondrial activity was significantly decreased in cells exposed to concentrations >200 μg/ml of nano-scale CeO_2 particles for 24 h. The rate of decrease was 10–20% compared with untreated cells. Reduction of cell viability was not observed when CeO_2 concentration was 100 μg/ml. There are two possibilities for the decrease in mitochondrial activity. One possibility is that, although cell membrane damage did not occur, mitochondrial dysfunction was induced by high concentration of CeO_2 nanoparticles. Another possibility is that synthesized formazan from MTT by mitochondrial dehydrogenase was adsorbed on CeO_2 nanoparticles and thus cell viability seemed to decrease. Actually, MTT assay is not suitable for carbon nanotube (CNT) because MTT formazan is adsorbed to CNT fiber and it does not dissolve (*23*).

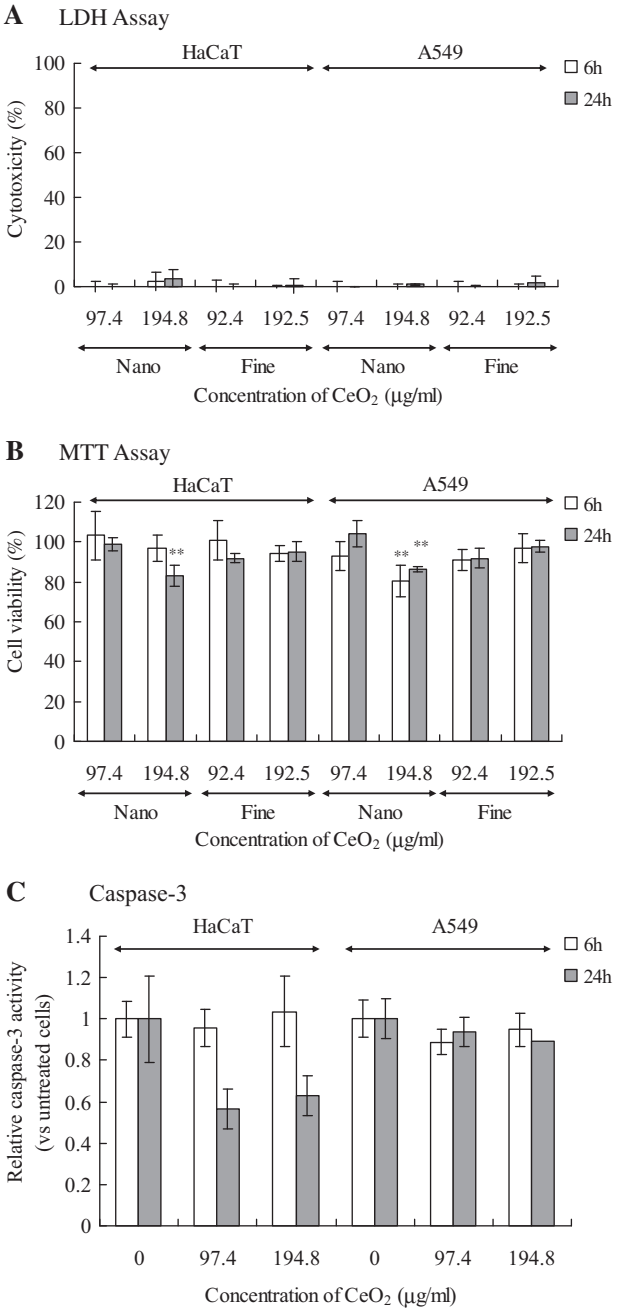

Fig. 1 Effect of the CeO_2–DMEM–FBS dispersion on cell viability. HaCaT cells and A549 cells were exposed to the CeO_2–DMEM–FBS dispersion. (A) Cells were treated with the dispersion for 6 and 24 h and cytotoxicity measured by the LDH assay. The method of calculating cytotoxicity is described in the Materials and Methods section. (B) Cells were treated with the dispersion for 6 and 24 h and viability measured by the MTT assay. The percentage of viable cells compared with the standardized control was 100%. (C) Caspase-3 activity in HaCaT cells exposed to nano-scale CeO_2–DMEM–FBS. Cell lysate samples were taken after cells were exposed to the CeO_2–DMEM–FBS dispersion for 6 and 24 h. Cell lysates were then subjected to caspase-3 activity assays. Caspase-3 activity was measured using DEVD-AFC as a substrate. $^{**}P < 0.01$ (Dunnett, ANOVA).

Caspase-3 activities in CeO_2 nanoparticles-exposed cells were also measured (Fig. 1C). Caspase-3 is a major apoptosis-related cysteine protease that is activated in apoptotic cells. Caspsase-3 activity did not increase in any CeO_2-exposed cells compared with untreated cells. This result indicates that a high concentration and long period of exposure of CeO_2 nanoparticles only slightly affects mitochondrial activity. CeO_2 particles did not cause cell death.

Influence of CeO_2 particles on cell proliferation

The influence of CeO_2 particles on cell proliferation was examined by a clonogenic assay (Fig. 2). Inhibition of cell proliferation was observed in cells exposed to 200 μg/ml of CeO_2 nanoparticles. Inhibitory effect was not observed in A549 cells. Fine CeO_2 particles did not inhibit cell proliferation in HaCaT cells or A549 cells.

Cellular uptake of CeO_2 particles

HaCaT cells exposed to nano-scale and fine CeO_2 particles were observed using TEM (Fig. 3). Uptake of CeO_2 particles into cells after 24-h exposure to nanoparticles and fine particles was also observed.

CeO_2 particles were detected in the cell cytoplasm. Invasion of CeO_2 particles into the nucleus was not observed. In the case of nanoparticles, intracellular CeO_2 nanoparticles were present as aggregates within phagosome-like structures. Intracellular fine particles were present alone or as aggregates of several particles. Sizes of intracellular CeO_2 aggregates approximately corresponded to those estimated from DLS measurements, but larger aggregates were also observed for nanoparticles. This observation suggests that several nanoparticles (including those inside of phagosomes) were accumulated. The cell-exposure concentration of nanoparticles and fine CeO_2 particles was similar, 118.3 and 120 μg/ml, respectively. The effect of primary particle size on cellular uptake was unclear, but

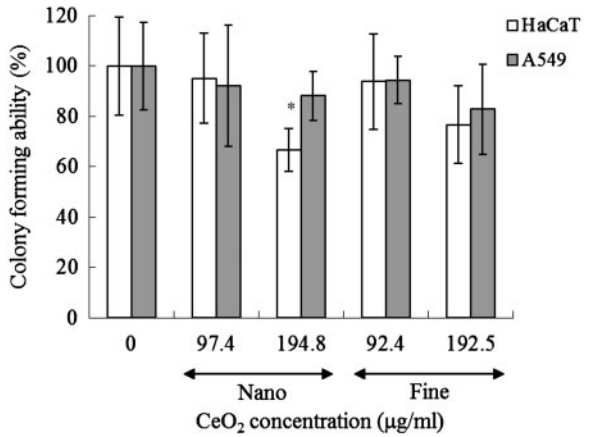

Fig. 2 Effect of the CeO_2–DMEM–FBS dispersion on cell proliferation. HaCaT cells and A549 cells were exposed to the CeO_2–DMEM–FBS dispersion. Cell proliferation was measured by the clonogenic assay. After the cells were cultured with the CeO_2–DMEM–FBS dispersion for 7 days, the number of colonies were counted. Cell proliferation standardized to control (100%). $^*P < 0.05$ (versus control, Dunnett, ANOVA).

there was a tendency for more nanoparticles than fine particles to be internalized within cells. We did not measure the mass of internalized CeO_2 in cells. Cellular uptake was observed at only 24-h exposure. Therefore, at this point, the distinction of kinetics of cellular uptake between nanoparticles and fine particles could not be ascertained.

Intracellular oxidative stress in cells exposed to CeO_2

Next, we examined the induction of intracellular oxidative stress by internalized CeO_2 cells. The CeO_2–DMEM–FBS dispersions of approximate concentration 100 and 200 μg/ml were applied to HaCaT cells and A549 cells. Intracellular levels of ROS were measured at 2, 6, 12 and 24 h (Fig. 4A). When CeO_2 nanoparticle concentration was 200 μg/ml, the intracellular level of ROS in cells exposed to nanoparticles for 24 h was increased to 1.3–1.5-times versus unexposed cells. In HaCaT cells and A549 cells, the intracellular ROS level was lowest at 6 h after exposure. When CeO_2 nanoparticle concentration was 100 μg/ml, there was no induction of intracellular ROS at any time point. When cells were exposed to CeO_2 nanoparticles for ≥6 h, the intracellular ROS level was significantly lower compared with unexposed cells. On the other hand, fine CeO_2 particles did not induce increase of intracellular ROS level at any time point and concentrations. The intracellular lipid peroxidation level was also measured (Fig. 4B). Cells exposed to CeO_2 nanoparticles for 24 h showed a tendency to increase the level of intracellular lipid peroxidation, but the difference was not significant. These results indicate that a high concentration (≤200 μg/ml) and/or long exposure (≤24 h) to CeO_2 nanoparticles leads to oxidative stress in cells, whereas a low concentration and/or short exposure to CeO_2 nanoparticles lead to anti-oxidative effects in cells.

Influence of Ca^{2+} adsorption on the surface of CeO_2 particles on cells

It has been reported that CeO_2 nanoparticles adsorbed culture-medium components such as proteins and Ca^{2+} (*17*). The ability of CeO_2 particles to adsorb protein and $Ca^{2+}$was therefore examined in the present study.

Both, nanoparticles and fine particles of CeO_2showed strong ability to adsorb Ca^{2+} (Fig. 5). On the other hand, although CeO_2 nanoparticles showed strong protein adsorption ability, CeO_2 fine particles hardly adsorbed proteins.

The cellular uptake of CeO_2 particles was shown, so the possibility of bringing Ca^{2+} into cells with CeO_2 particles was examined. The intracellular Ca^{2+} concentration in CeO_2-exposed cells was measured by Fluo 4. When cells were exposed to both the CeO_2 nanoparticles and the fine-scale particles, the intracellular Ca^{2+} concentration was higher than that of unexposed cells (Fig. 6A).

Observations of CeO2 exposure cells by confocal laser microscope also showed increase of intracellular Ca^{2+} level (Fig. 6B). Fluorescence of fluo 4 was observed at cytosol. Particularly, in CeO_2 fine-particle

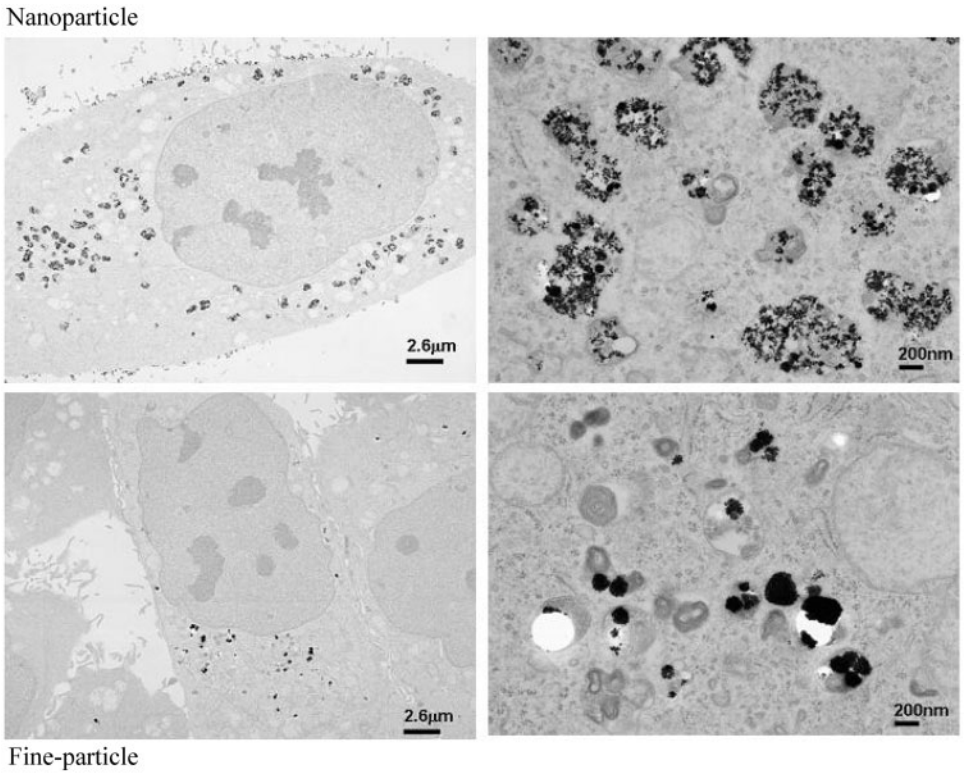

Fig. 3 Transmission electron microscope observations of cells exposed to CeO_2 particles. HaCaT cells were exposed to the CeO_2–DMEM–FBS dispersion for 24 h. The upper figure shows nanoparticle-exposed cells and the lower figure shows cells exposed to fine particles. CeO_2 concentrations in nano-scale and fine CeO_2 dispersions were 118.3 μg/ml and 120 μg/ml, respectively.

exposed cells, the fluorescence was overlapped to the image of aggregated particle-like structure.

Moreover, exposure of CeO_2 nanoparticles at ≤200 μg/ml for 24 h induced an increase in activity of the Ca^{2+}-dependent cysteine protease calpain (Fig. 7). On the other hand, calpain activation were not found in fine-particle exposed cells. These results suggested that CeO_2 nanoparticles led to an increase in intracellular Ca^{2+} concentration due to their ability to adsorb and uptake Ca^{2+}.

Discussion

In this study, we assessed cellular influences induced by stable CeO_2 nanoparticles in culture medium dispersion. Exposure of CeO_2 nanoparticles to cultured cells induced some cellular effects. When cells were exposed to CeO_2 nanoparticles at ~200 μg/ml for 24 h, the intracellular ROS level was increased and mitochondrial activity slightly decreased. In HaCaT cells, CeO_2 nanoparticles inhibited colony-forming ability. Injury of cell membrane did not occur. Cellular uptake was observed not only for nanoparticles, but also for fine particles. Cellular uptake of CeO_2 particles was therefore not specific to nanoparticles. Although nanoparticles and fine particles were taken up into cells, cellular influences were stronger in CeO_2 nanoparticles than in fine particles. Fine CeO_2 particles had virtually no influence on cells. Generally, it is explained that strong cellular influences of nanoparticles are caused by larger specific surface area than that of fine particles. However, specific surface area of fine CeO_2 particles used in this study was larger than nanoparticles.

The increase of the oxidative stress by CeO_2 nanoparticles has already been reported. Lin *et al.* (*13*) reported that CeO_2 nanoparticles induced oxidative stress to A549 cells at an exposure condition of 3.5, 10.5 and 23.3 μg/ml for 24, 48 and 72 h. Induction of intracellular ROS level and decrease of cell viability were caused with time dependency by CeO_2 nanoparticle exposure, in this case the exposure condition was 5, 10, 20 and 40 μg/ml for 24, 48, 72 and 96 h (*14*). On the other hand, it is also reported that CeO2 nanoparticles showed anti-oxidative activity and had no influence to the cell viability, in this case the exposure condition was 25 μg/ml for 1–16 h (*9*).

In this study, intracellular ROS level was increased in cells exposed to 200 μg/ml of CeO_2 for 24 h. The increase in intracellular ROS level of CeO_2-exposed cells was ~1.5-times that of untreated cells. However, this increase was weaker than that of other metal oxide nanoparticles that induce oxidative stress (e.g., ZnO, CuO) (*3*, *9*, *24*). Cytotoxic metal oxide nanoparticles such as CuO, ZnO and NiO, released metal ion in the culture medium. Their cytotoxicity was influenced by their solubility (*1*, *3*, *25*, *26*). In the present study, CeO_2 nanoparticles and CeO_2 fine particles did not dissolve in the culture medium. Thus, there is no possibility that the cellular effects caused by CeO_2 nanoparticles were induced by release of the ceric ion.

Moreover, when the CeO_2 concentration was 100 μg/ml, the intracellular ROS level was decreased compared with untreated cells. As described above,

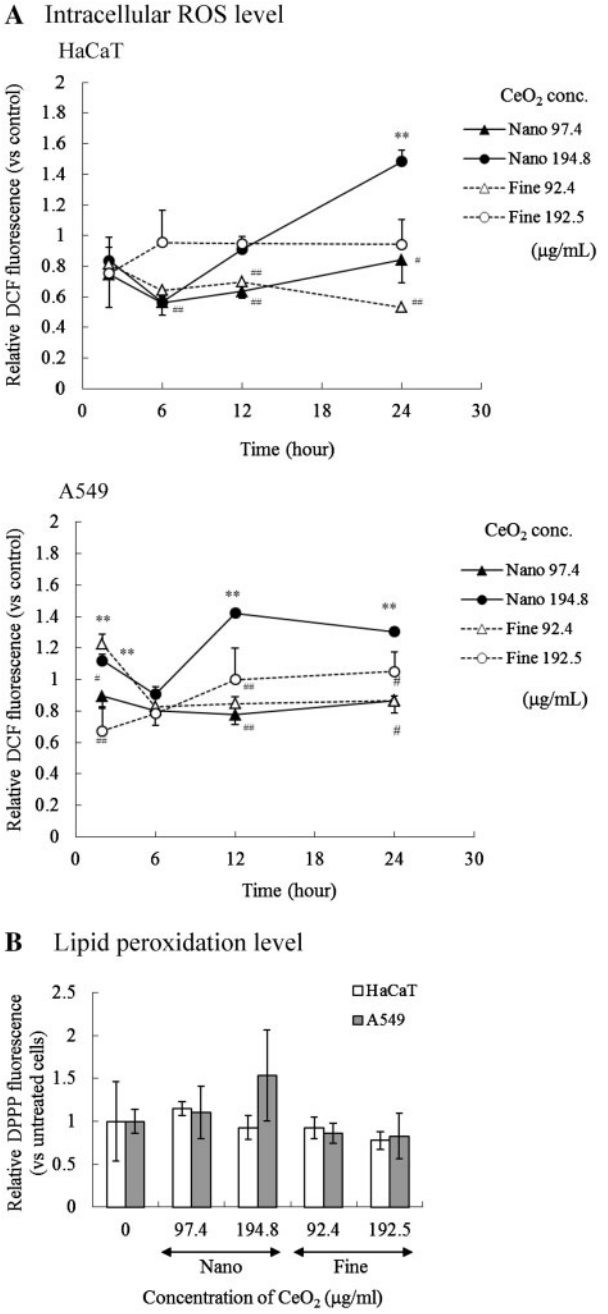

Fig. 4 Oxidative stress level in CeO_2-exposed cells. (A) Intracellular ROS level in HaCaT cells and A549 cells exposed to nano-scale CeO_2–DMEM–FBS. Cells were exposed to CeO_2–DMEM–FBS dispersions for 2, 6, 12 and 24 h. Then, the medium was exchanged with fresh, FBS-free DMEM containing 10 μM of DCFH-DA. After incubation for 30 min, cells were collected and washed. DCFH fluorescence in cells was measured by flow cytometry. The value of DCFH fluorescence-standardized untreated cells was 1. $^{**}P<0.01$ (significantly high versus untreated cells, Dunnett, ANOVA). $^{\#}P<0.05$, $^{\#\#}P<0.01$ (significantly low versus untreated cells, Dunnett, ANOVA). (B) Intracellular lipid peroxide level in cells exposed to nano-scale CeO_2–DMEM–FBS. Cells were exposed to nano-scale and fine CeO_2–DMEM–FBS dispersions for 24 h. After incubation, the intracellular lipid peroxidation level was measured using DPPP.

there are contradictory results that CeO_2 nanoparticles induced oxidative stress in cells (*13*, *14*) and that CeO_2 showed an anti-oxidative stress effect (*8*, *9*). In the present study, the influence of CeO_2 on the intracellular

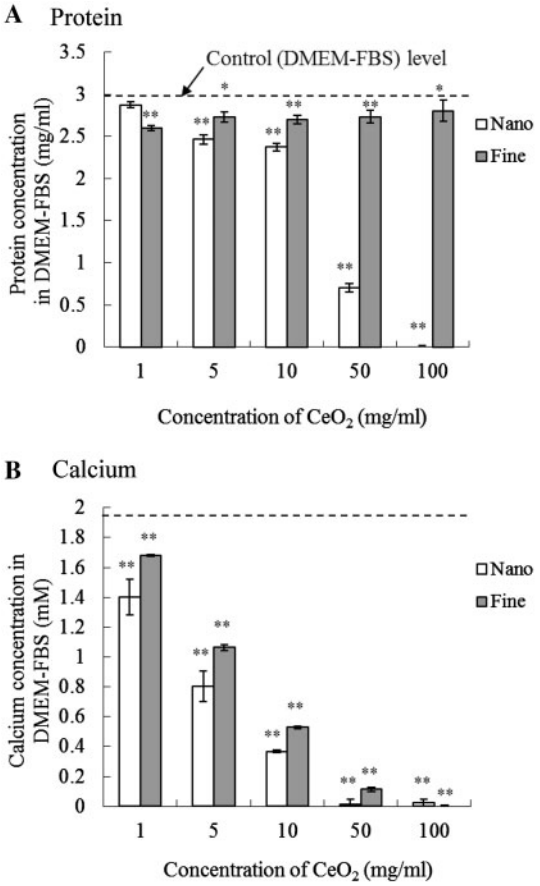

Fig. 5 Protein and calcium adsorption ability of CeO_2 particles. (A) Protein adsorption of CeO_2 particles. TheCeO_2 particles were dispersed in DMEM–FBS by various concentrations. After the centrifugation, the unadsorbed protein concentration in supernatant was measured. DMEM–FBS which does not contain any CeO_2 was used as control. (B) Calcium adsorption of metal oxides. The un-adsorbed calcium concentration of the same sample as (A) was measured by OCPC method.

ROS level was dependent upon CeO_2 concentration and exposure time. In the case of 24-h exposure, 200 μg/ml of CeO_2 nanoparticles induced an increase in the intracellular ROS level; but 100 μg/ml of CeO_2 nanoparticles induced a decrease in the intracellular ROS level. In the case of 6-h exposure, the intracellular ROS level was decreased even if CeO_2 concentration was 200 μg/ml. These results suggest that CeO_2 could induce oxidative stress in culture cells.

Essentially, CeO_2 is an insoluble and inactive particle. However, CeO_2 nanoparticles had cellular influences. The ability of CeO_2 to induce oxidative stress was not strong; a low concentration or short duration of exposure would drive the activation of an anti-oxidative system in the cell. It has been reported that expression of HO-1 (a major stress response enzyme, known to decrease oxidative stress) was increased by exposure to CeO_2 nanoparticles (*12*). Therefore, it can be inferred that cells get a temporary resistance to oxidative stress. However, long-term or high concentration exposure would induce dysfunction of anti-oxidative systems such as depletion of GSH and thus the level of oxidative stress changed to an increase.

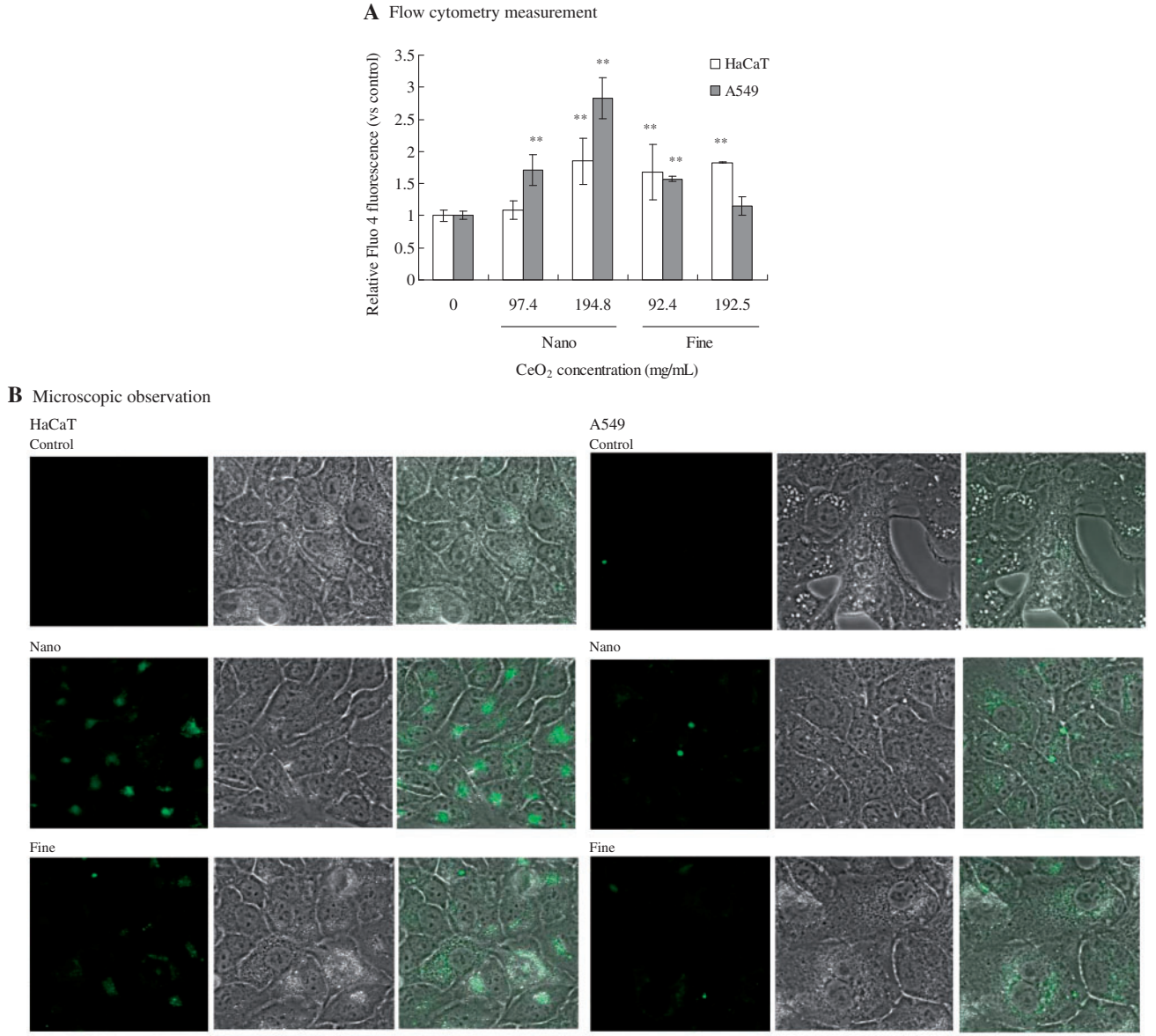

Fig. 6 Intracellular Ca^{2+} level in HaCaT cells and A549 cells exposed to nano-scale CeO_2–DMEM–FBS. (A) Cells were exposed to CeO_2–DMEM–FBS dispersions for 24 h. Then, the medium was exchanged with fresh, FBS-free DMEM containing 5 μg/ml of Fluo 4-AM. After incubation for 1 h, cells were collected and washed. Fluo 4 fluorescence in cells was measured by flow cytometry. The value of Fluo 4 fluorescence-standardized untreated cells was 1. $^{**}P<0.01$ (versus untreated cells, Dunnett, ANOVA). (B) Observation of fluo 4 staining CeO_2 exposed cells by confocal laser microscope. Excitation and emission wavelengths were 494 and 516 nm, respectively.

Results of the present study and previous studies (*13*, *14*) indicate a possibility that long term exposure of CeO_2 nanoparticles induce oxidative stress and cell death including apoptosis to cultured cells. Inconsistent results of former investigations might have been caused by bilateral character of CeO_2 nanoparticles. Therefore, exposure time and concentration are important factors for *in vitro* assessment of cellular influences induced by inactive nanoparticles such as CeO_2. Additionally, CeO_2 nanoparticles directly dispersed into culture medium form large aggregates and agglomerates. The CeO_2 concentration in an unstable medium dispersion does not reflect the cell exposure concentration because large aggregates/agglomerates accumulate on the cell. Moreover, the physical and chemical properties of CeO_2 nanoparticles produced by different manufacturer will be different, even if it has the same name 'CeO_2'. Physical and chemical properties, at least primary particle size, specific surface area, purity, solubility, secondary particle size and dispersion stability are essential for *in vitro* evaluation of cellular influences of CeO_2 nanoparticles. Actually, the question fell upon why CeO_2 nanoparticles have a greater effect on cells than fine particles.

The present study also revealed that CeO_2 nanoparticles have strong protein and Ca^{2+} adsorption ability. In particular, the ability to adsorb Ca^{2+} is strong. Ca^{2+} is an important element for cell signalling pathways and some enzymatic activities in cells and the

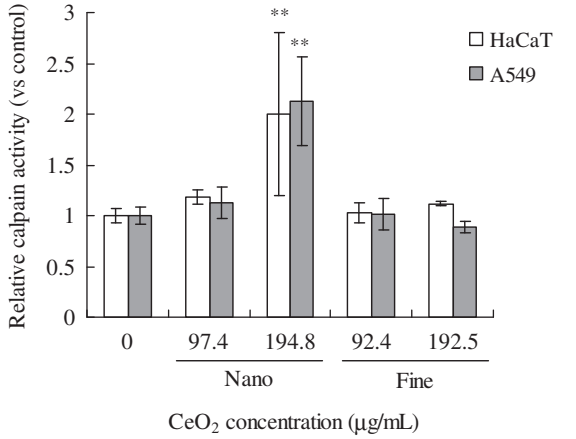

Fig. 7 Calpain activity in HaCaT cells exposed to nano-scale CeO_2–DMEM–FBS. Cell lysate samples were taken after cells were exposed to the CeO_2–DMEM–FBS dispersion for 24 h. Cell lysates were then subjected to calpain activity assays. Calpain activity was measured using Ac-LLY-conjugated AFC as a substrate. $*P<0.05$; $**P<0.01$ (versus untreated cells, Dunnett, ANOVA).

intracellular Ca^{2+} is very tightly controlled. In healthy cells, Ca^{2+} concentration is kept very low in intracellular fluids. Influx of Ca^{2+} from extracellular sources and release of Ca^{2+} from the endoplasmic reticulum to the intracellular *milieu* has significant physiological effects. In the present study, the possibility that CeO_2 nanoparticles bring Ca^{2+} into cells due to their Ca^{2+} adsorption ability is suggested. Internalized CeO_2 nanoparticles will release Ca^{2+} into intracellular fluid. As a result, intracellular Ca^{2+} concentration increases in CeO_2 nanoparticle-exposed cells and the increase in intracellular Ca^{2+} affects cell signalling pathways. Calpain was activated in CeO_2 nanoparticle-exposed cells. Calpain is a Ca^{2+}-dependent cysteine protease (*27*). Additionally, it is reported that calpain activation was involved in apoptotic cell death (*28*). However, calpain function is incompletely understood. Moreover, there are other Ca^{2+}-dependent molecules in the cell. For example, calmodulin is involved in cell signalling (*29*) and cadherin is involved in cell adhesion (*30*, *31*). These Ca^{2+}-dependent proteins are important for cellular homeostasis. Therefore, there is a possibility that increase in intracellular Ca^{2+} concentration induced by CeO_2 nanoparticles leads to disruption of Ca^{2+}-dependent molecules.

On the other hand, CeO_2 fine particles also adsorbed Ca^{2+} and intracellular Ca^{2+} was increased in CeO_2 fine-particle exposed cells. However, increase of calpain activity was not observed. Confocal laser microscopic observations showed that fluo 4 fluorescence overlapped to the image of aggregated particulate-like structure in fine-particle exposed cells. This observation suggests the possibility that Ca^{2+} was adsorbed on the surface of fine CeO_2 particles. It is reported that TiO_2 particles adsorbed Ca^{2+} via albumin. Serum albumin, the predominant serum protein, is a Ca^{2+} binding protein, however, the Ca^{2+} binding ability is not strong. Compared with CeO_2 nanoparticles that showed a strong protein adsorption ability, CeO_2 fine particles hardly adsorbed proteins. These results suggest a possibility that CeO_2 nanoparticles and fine particles adsorbed Ca^{2+} by different mechanisms. CeO_2 nanoparticles adsorb Ca^{2+} via serum albumin and CeO_2 fine particles bind to Ca^{2+} directly. In fine CeO_2 particles, Ca^{2+} may stay on the surface. Another possibility of intracellular Ca^{2+} induction is that, CeO_2 nanoparticles enhance Ca^{2+} influx. It has been reported that ZnO is strongly cytotoxic and induced oxidative stress and increase in intracellular Ca^{2+} concentration in cells (*24*).

CeO_2 exposure at higher concentration (200 μg/ml) for 24 h to cells induced increase of intracellular ROS and Ca^{2+} levels and activation of calpain. However, induction of intracellular Ca^{2+} was also observed in fine CeO_2 particle exposed cells without increase in intracellular ROS level. Additionally, hydrogen peroxide induced oxidative stress in cells but did not increase the intracellular Ca^{2+} concentration (data not shown). Therefore, increase of intracellular ROS is not a direct trigger of increase in intracellular Ca^{2+}. Weber *et al.* (*32*) reported that induction of oxidative stress by H_2O_2-induced calpain activation and subsequent LDH release in cultured pancreatic acinar cells. In this study, calpain was only activated in CeO_2 nanoparticle exposed cells at concentration of 200 mg/ml. At the present time, association among intracellular ROS, calcium concentration and calpain activity is not clear. CeO_2 nanoparticles adsorb not only Ca^{2+} but also proteins and other medium components. Therefore, CeO_2 nanoparticles can also import foreign proteins (e.g. serum albumin) into the cell. Such foreign proteins could be associated with an increase in intracellular ROS concentration. Details of intracellular Ca^{2+} induction mechanism are still unclear. In order to understand the mechanism of increase of intracellular Ca^{2+} by CeO_2 nanoparticle, further examinations are required. In the present study, CeO_2 nanoparticles showed some cellular influences *in vitro*. Two important cellular influences were suggested: (i) increase in intracellular Ca^{2+} concentration (possibly caused by the Ca^{2+} adsorption ability of CeO_2 nanoparticles) and (ii) induction of oxidative stress in cells. Although these influences were small, secondary effects such as inhibition of colony formation and decrease in cell viability will result at high concentrations of CeO_2.

On the other hand, there is a possibility that these cellular influences, increase of intracellular Ca^{2+} and ROS levels are artificial effects because cell culture medium contains many proteins and salts and these components are adsorbed to CeO_2 nanoparticles. There is a more complex defensive system against oxidative stress *in vivo*. Therefore, the influence of CeO_2 in animals will be slight. However, the possibility that CeO_2 nanoparticles cause local effects, such as an induction of oxidative stress cannot be ignored. For thorough evaluation of the *in vivo* influence of CeO_2 nanoparticles, examination in animals is essential. The clearance of CeO_2 particles is an important factor in biological effects *in vivo*.

Acknowledgements

We would like to thank Ms Emiko Kobayashi (National Institute of Advanced Industrial Science and Technology, Japan) for help in performing the TEM observations.

Funding

New Energy and Industrial Technology Development Organization of Japan (NEDO) [Grant 'Evaluating risks associated with manufactured nanomaterials (P06041)'].

Conflict of interest

None declared.

References

1. Horie, M., Nishio, K., Fujita, K., Kato, H., Nakamura, A., Kinugasa, S., Endoh, S., Miyauchi, A., Yamamoto, K., Murayama, H., Niki, E., Iwahashi, H., Yoshida, Y., and Nakanishi, J. (2009) Ultrafine NiO particles induce cytotoxicity in vitro by cellular uptake and subsequent Ni(II) release. *Chem. Res. Toxicol.* **22**, 1415–1426
2. Lu, S., Duffin, R., Poland, C., Daly, P., Murphy, F., Drost, E., Macnee, W., Stone, V., and Donaldson, K. (2009) Efficacy of simple short-term in vitro assays for predicting the potential of metal oxide nanoparticles to cause pulmonary inflammation. *Environ. Health Perspect.* **117**, 241–247
3. Karlsson, H.L., Cronholm, P., Gustafsson, J., and Möller, L. (2008) Copper oxide nanoparticles are highly toxic: a comparison between metal oxide nanoparticles and carbon nanotubes. *Chem. Res. Toxicol.* **21**, 1726–1732
4. Fahmy, B. and Cormier, S.A. (2009) Copper oxide nanoparticles induce oxidative stress and cytotoxicity in airway epithelial cells. *Toxicol. In Vitro* **23**, 1365–1371
5. Park, B., Donaldson, K., Duffin, R., Tran, L., Kelly, F., Mudway, I., Morin, J.P., Guest, R., Jenkinson, P., Samaras, Z., Giannouli, M., Kouridis, H., and Martin, P. (2008) Hazard and risk assessment of a nanoparticulate cerium oxide-based diesel fuel additive - a case study. *Inhal. Toxicol.* **20**, 547–566
6. Park, B., Martin, P., Harris, C., Guest, R., Whittingham, A., Jenkinson, P., and Handley, J. (2007) Initial in vitro screening approach to investigate the potential health and environmental hazards of Envirox^{TM} - a nanoparticulate cerium oxide diesel fuel additive. *Part. Fibre Toxicol.* **4**, 12
7. Pierscionek, B.K., Li, Y., Yasseen, A.A., Colhoun, L.M., Schachar, R.A., and Chen, W. (2010) Nanoceria have no genotoxic effect on human lens epithelial cells. *Nanotechnology* **21**, 035102
8. Schubert, D., Dargusch, R., Raitano, J., and Chan, S.W. (2006) Cerium and yttrium oxide nanoparticles are neuroprotective. *Biochem. Biophys. Res. Commun.* **342**, 86–91
9. Xia, T., Kovochich, M., Liong, M., Mädler, L., Gilbert, B., Shi, H., Yeh, J.I., Zink, J.I., and Nel, A.E. (2008) Comparison of the mechanism of toxicity of zinc oxide and cerium oxide nanoparticles based on dissolution and oxidative stress properties. *ACS Nano* **2**, 2121–2134
10. Heckert, E.G., Karakoti, A.S., Seal, S., and Self, W.T. (2008) The role of cerium redox state in the SOD mimetic activity of nanoceria. *Biomaterials* **29**, 2705–2709
11. Hirst, S.M., Karakoti, A.S., Tyler, R.D., Sriranganathan, N., Seal, S., and Reilly, C.M. (2009) Anti-inflammatory properties of cerium oxide nanoparticles. *Small* **5**, 2848–2856
12. Eom, H.J. and Choi, J. (2009) Oxidative stress of CeO_2 nanoparticles via p38-Nrf-2 signaling pathway in human bronchial epithelial cell, Beas-2B. *Toxicol. Lett.* **187**, 77–83
13. Lin, W., Huang, Y.W., Zhou, X.D., and Ma, Y. (2006) Toxicity of cerium oxide nanoparticles in human lung cancer cells. *Int. J. Toxicol.* **25**, 451–457
14. Park, E.J., Choi, J., Park, Y.K., and Park, K. (2008) Oxidative stress induced by cerium oxide nanoparticles in cultured BEAS-2B cells. *Toxicology* **245**, 90–100
15. Thill, A., Zeyons, O., Spalla, O., Chauvat, F., Rose, J., Auffan, M., and Flank, A.M. (2006) Cytotoxicity of CeO_2 nanoparticles for Escherichia coli. Physico-chemical insight of the cytotoxicity mechanism. *Environ. Sci. Technol.* **40**, 6151–6156
16. Niki, E. (2007) Eustress and distress. *Nippon Yakurigaku Zasshi* **129**, 76–79
17. Horie, M., Nishio, K., Fujita, K., Endoh, S., Miyauchi, A., Saito, Y., Iwahashi, H., Yamamoto, K., Murayama, H., Nakano, H., Nanashima, N., Niki, E., and Yoshida, Y. (2009) Protein adsorption of ultrafine metal oxide and its influence on cytotoxicity toward cultured cells. *Chem. Res. Toxicol.* **22**, 543–553
18. Kato, H., Suzuki, M., Fujita, K., Horie, M., Endoh, S., Yoshida, Y., Iwahashi, H., Takahashi, K., Nakamura, A., and Kinugasa, S. (2009) Reliable size determination of nanoparticles using dynamic light scattering method for in vitro toxicology assessment. *Toxicol. In Vitro* **23**, 927–934
19. Kato, H., Fujita, K., Horie, M., Suzuki, M., Nakamura, A., Endoh, S., Yoshida, Y., Iwahashi, H., Takahashi, K., and Kinugasa, S. (2010) Dispersion characteristics of various metal oxide secondary nanoparticles in culture medium for in vitro toxicology assessment. *Toxicol. In Vitro* **24**, 1009–1018
20. Herzog, E., Casey, A., Lyng, F.M., Chambers, G., Byrne, H.J., and Davoren, M. (2007) A new approach to the toxicity testing of carbon-based nanomaterials–the clonogenic assay. *Toxicol. Lett.* **174**, 49–60
21. Franken, N.A., Rodermond, H.M., Stap, J., Haveman, J., and van Bree, C. (2006) Clonogenic assay of cells in vitro. *Nat. Protoc.* **1**, 2315–2319
22. Okimoto, Y., Watanabe, A., Niki, E., Yamashita, T, and Noguchi, N. (2000) A novel fluorescent p diphenylpyrenylphosphine to follow lipid peroxidation in cell membranes. *FEBS Lett.* **474**, 137–140
23. Wörle-Knirsch, J.M., Pulskamp, K., and Krug, H.F. (2006) Oops they did it again! Carbon nanotubes hoax scientists in viability assays. *Nano Lett.* **6**, 1261–1268
24. Huang, C.C., Aronstam, R.S., Chen, D.R., and Huang, Y.W. (2010) Oxidative stress, calcium homeostasis, and altered gene expression in human lung epithelial cells exposed to ZnO nanoparticles. *Toxicol. In Vitro* **24**, 45–55
25. Horie, M., Fukui, H., Nishio, K., Endoh, S., Kato, H., Fujita, K., Miyauchi, A., Nakamura, A., Shichiri, M., Ishida, N., Kinugasa, S., Morimoto, Y., Niki, E., Yoshida, Y., and Iwahashi, H. (2011) Evaluation of acute oxidative stress induced by NiO nanoparticles in vivo and in vitro. *J. Occup. Health* **53**, 64–74
26. Forti, E., Salovaara, S., Cetin, Y., Bulgheroni, A., Tessadri, R., Jennings, P., Pfaller, W., and Prieto, P. (2011) In vitro evaluation of the toxicity induced by nickel soluble and particulate forms in human airway epithelial cells. *Toxicol. in Vitro* **25**, 454–461
27. Murachi, T. (1984) Calcium-dependent proteinases and specific inhibitors: calpain and calpastatin. *Biochem. Soc. Symp.* **49**, 149–167

28. Cao, G., Xing, J., Xiao, X., Liou, A.K., Gao, Y., Yin, X.M., Clark, R.S., Graham, S.H., and Chen, J. (2007) Critical role of calpain I in mitochondrial release of apoptosis-inducing factor in ischemic neuronal injury. *J. Neurosci.* **27**, 9278–9293
29. Swulius, M.T. and Waxham, M.N. (2008) Ca(2+)/calmodulin-dependent protein kinases. *Cell Mol. Life Sci.* **65**, 2637–2657
30. Takeichi, M. (1988) The cadherins: cell-cell adhesion molecules controlling animal morphogenesis. *Development* **102**, 639–655
31. van Roy, F. and Berx, G. (2008) The cell-cell adhesion molecule E-cadherin. *Cell Mol. Life Sci.* **65**, 3756–3788
32. Weber, H., Hühns, S., Lüthen, F., Jonas, L., and Schuff-Werner, P. (2005) Calpain activation contributes to oxidative stress-induced pancreatic acinar cell injury. *Biochem. Pharmacol.* **70**, 1241–1252